

Kinetochores-driven formation of kinetochore fibers contributes to spindle assembly during animal mitosis

Helder Maiato,¹ Conly L. Rieder,^{1,2,3} and Alexey Khodjakov^{1,2,3}

¹Wadsworth Center, New York State Department of Health, Albany, NY 12201

²Department of Biomedical Sciences, State University of New York, Albany, NY 12222

³Marine Biological Laboratory, Woods Hole, MA 02543

It is now clear that a centrosome-independent pathway for mitotic spindle assembly exists even in cells that normally possess centrosomes. The question remains, however, whether this pathway only activates when centrosome activity is compromised, or whether it contributes to spindle morphogenesis during a normal mitosis. Here, we show that many of the kinetochore fibers (K-fibers) in centrosomal *Drosophila* S2 cells are formed by the kinetochores. Initially, kinetochore-formed K-fibers are not oriented toward a spindle pole but, as they grow, their minus ends are captured by astral microtubules (MTs) and

transported poleward through a dynein-dependent mechanism. This poleward transport results in chromosome bi-orientation and congression. Furthermore, when individual K-fibers are severed by laser microsurgery, they regrow from the kinetochore outward via MT plus-end polymerization at the kinetochore. Thus, even in the presence of centrosomes, the formation of some K-fibers is initiated by the kinetochores. However, centrosomes facilitate the proper orientation of K-fibers toward spindle poles by integrating them into a common spindle.

Introduction

Depending on the organism, spindle assembly during mitosis can occur via two distinct pathways. In cells that contain centrosomes, these organelles generate arrays of highly dynamic astral microtubules (MTs), which explore the cytoplasm, searching for chromosomes. When an astral MT encounters a specialized structure on the chromosome's primary constriction—the kinetochore—it is captured and stabilized (Kirschner and Mitchison, 1986). Selective stabilization of captured MTs results in the formation of the typical fusiform spindle in which the poles are focused on the centrosomes. The capture of a single astral MT by a kinetochore has been visualized directly in newt lung cultures (Hayden et al., 1990; Rieder and Alexander, 1990), demonstrating the existence of this mechanism in vertebrate somatic cells. After the initial MT capture, kinetochores develop a bundle of 15–30 parallel MTs that connect them to spindle poles. It is generally assumed that these bundles, termed kinetochore fibers (K-fibers), are formed via repetitive MT capture, however this mechanism has not been directly validated (McEwen et al., 1997).

The search-and-capture mechanism is not relevant to spindle assembly in cells lacking centrosomes, which include higher plants and some animal oocytes. In these cells formation of an acentrosomal spindle begins with the nucleation of MTs in the vicinity of the chromosomes via a process that likely involves Ran/RCC1 activity (Karsenti and Vernos, 2001; Li et al., 2003).

For years, the centrosomal and acentrosomal routes of spindle formation have been viewed as mutually exclusive pathways, in that any given cell is thought to use one or the other, but not both mechanisms. However, recent studies have clearly demonstrated that animal cells, which normally contain centrosomes, still form a functional bipolar spindle after these organelles are removed (Khodjakov et al., 2000; Hinchcliffe et al., 2001). Furthermore, *Drosophila* mutants that appear to lack a functional centrosome undergo a normal mitosis (Bonaccorsi et al., 1998; Megraw et al., 2001). Thus, a centrosome-independent pathway for spindle assembly exists, even in cells that normally use centrosomes for this process. Yet, the question remains whether the acentrosomal pathway is activated only when cells cannot use their “normal” centrosome-mediated mechanism, or whether it is constitutively active, and contributes toward spindle morphogenesis even in the presence of cen-

Correspondence to Alexey Khodjakov: khodj@wadsworth.org

Abbreviations used in this paper: K-fiber, kinetochore fiber; MT, microtubule; NEB, nuclear envelope breakdown.

trosomes. If the latter is true, then some of the K-fibers in animal cells that contain centrosomes should be generated via a centrosome-independent mechanism, even when centrosomes are present and functionally active.

The major impediment to direct evaluation of how individual K-fibers form in animal cells is that the chromosomes normally reside, at the start of spindle assembly, between two massive astral MT arrays generated by the separated centrosomes. The number of dynamic MTs, and the speed with which they penetrate the space around chromosomes at nuclear envelope breakdown (NEB), make it impossible to clearly resolve individual K-fibers, yet alone follow their formation. Observations on cells recovering from MT poisons (Witt et al., 1980; De Brabander et al., 1981; Czaban and Forer, 1985) or low temperature (Inoue, 1964; Bajer, 1987) suggest that kinetochores can promote MT nucleation *in vivo*. However, the physiological relevance of these observations has been challenged, on the grounds that the complete disassembly of MTs significantly increases the pool of soluble tubulin, which could lead to MT nucleation at sites that are normally not involved in this process under physiological conditions (Pickett-Heaps et al., 1982). Thus, although these studies support the notion that kinetochores can nucleate/organize MTs independent of the centrosome in animal cells, it remains to be determined whether they do so during a normal mitosis.

More recently, Khodjakov and coworkers (Khodjakov et al., 2003) used monastrol, an Eg5-kinesin inhibitor, to arrest vertebrate cells in mitosis with monopolar spindles. In these spindles, the chromosomes encircle the unseparated centrosomes and the distal kinetochores on each chromosome, which face away from the single centrosome region, are therefore shielded from centrosome-generated MTs by the chromosomes themselves. Surprisingly, under this condition the distal kinetochores were seen to organize K-fibers. Furthermore, once formed, the free distal ends of these K-fibers were then transported toward the centrosome (i.e., the region of the spindle pole) along astral MTs. These data demonstrated that K-fibers can be organized via centrosome-independent mechanisms in

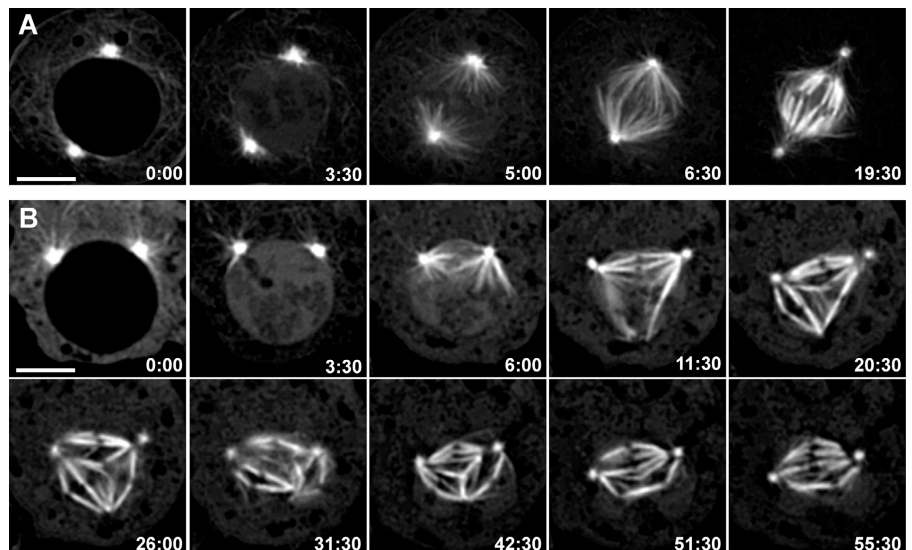
centrosome-containing cells, however, the origin of these K-fibers was not determined (Khodjakov et al., 2003).

Here, we demonstrate that kinetochores facing away from a centrosome often form K-fibers *de novo*. These observations are made in untreated *Drosophila* S2 cells expressing GFP/ α -tubulin (Goshima and Vale, 2003) that undergo a normal mitosis, and thus they reflect a normal physiological activity. As shown by others, when K-fibers are severed with a laser microbeam they regrow from the kinetochore outward. Importantly, we demonstrate that this growth in S2 cells occurs via MT plus-end polymerization at the kinetochore. K-fibers that are organized by kinetochores are not initially oriented toward a spindle pole (centrosome). Rather, they grow away from the kinetochore until their minus ends are captured and transported poleward along astral MTs, just as in monastrol-treated cells (Khodjakov et al., 2003). Dynein RNAi reveals that the capture and incorporation of K-fibers into a common half-spindle requires dynein activity. Together, our data reveal that kinetochore-driven K-fiber formation is a major mechanism that contributes toward spindle assembly during normal mitosis in centrosomal cells. However, integration of these kinetochore-organized K-fibers into the common spindle is facilitated by the centrosomes via a dynein-dependent search-and-capture.

Results

Drosophila tissue culture cells provide several advantages for studying spindle formation. They contain fewer chromosomes than most animal cells, and whereas K-fibers are strikingly robust there are relatively few astral MTs. The major disadvantage is that most *Drosophila* cell lines are semi-adherent and thus the cells are round, making high resolution microscopy difficult. To overcome this problem we have modified the agar-overlay technique recently described by Fleming and Rieder (2003) so that we can control the degree of cell flattening. Unlike cells flattened by growing on a Con A substrate (Rogers et al., 2002), the agar overlay approach allows one to select cells that are sufficiently flattened to be imaged at high spatial and

Figure 1. Spindle formation in *Drosophila* S2 cells stably expressing GFP/ α -tubulin. Selected frames from fluorescence microscopy time-lapse sequences of mitotic spindle formation in S2 cells. (A) Spindle formation in a cell with centrosomes completely separated before NEB. Note the rapid penetration of astral MTs inside the nucleus and the process of maturation of the K-fibers. (B) Spindle formation in a cell with centrosomes only partially separated by NEB. Note that formation of K-fibers is initially seen only on the side of chromosomes that face the centrosomes. However, within just a few minutes (compare 6:00 with 11:30), prominent K-fibers appear in association with those kinetochores that are oriented away from the centrosomes. These K-fibers converge and form an ectopic pole (20:30–26:00). However, over time, all distal K-fibers become incorporated into the main spindle that forms between the centrosomes (31:30–55:30). Time is in min:s. Bars, 5 μ m.



temporal resolution without compromising the ability of the cell to progress through mitosis and undergo normal cytokinesis. This feature makes it possible to discern individual K-fibers in fluorescence recordings throughout mitosis. All experiments reported here were conducted on S2 cells that stably express GFP/ α -tubulin (Goshima and Vale, 2003).

During mitosis some K-fibers are organized by the kinetochores in S2 cells

A common feature of mitosis in animals is that the two centrosomes can be at different stages of separation at the time of NEB (for review see Rieder, 1991). However, regardless of the relative positions of the centrosomes at NEB, a normal bipolar spindle ultimately forms. As originally reported (Goshima and Vale, 2003), *Drosophila* S2 cells used in this study frequently contain more than two centrosomes during prophase. These centrosomes are easily detectable in live cells as they generate pronounced MT asters. This feature allowed us to select cells with only two asters at NEB for our time-lapse recordings. Among 14 cells followed through mitosis, six had centrosomes positioned on opposite sides of the nucleus at NEB (Fig. 1 A). By contrast, in the other eight cells NEB occurred while the centrosomes were still relatively close to one another (Fig. 1 B).

In cells where centrosome separation was complete before NEB, astral MTs emanating from both centrosomes rapidly penetrated the region of the former nucleus, making it impossible to follow in detail the formation of individual K-fibers (Fig. 1 A and Video 1, available at <http://www.jcb.org/cgi/content/full/jcb.200407090/DC1>). In these cells most chromosomes congressed to the metaphase plate and spindle formation was completed within ~ 15 min after NEB.

In those cells where centrosome separation was incomplete at the time of NEB, many chromosomes were positioned at NEB outside of the region saturated with astral MTs. Nevertheless, these chromosomes consistently developed K-fibers on those kinetochores that faced away from the centrosomes, and were thus shielded from astral MTs by the chromosome body (Fig. 1 B and Video 2). These "distal" K-fibers were observed in all eight cells, and they first appeared in the vicinity of the kinetochore (Fig. 2 and Video 3) and then extended outward away from the centromere region. It was not unusual in cells that contained multiple distal K-fibers, for the ends of the fibers

to join to form an additional spindle pole lacking a centrosome (Fig. 1 B). This configuration was usually transient as, one by one the chromosomes became incorporated into a single bipolar spindle as the ends of their distal kinetochore K-fibers moved toward one of the centrosomal spindle poles. After all K-fibers were incorporated into a bipolar spindle (Fig. 1 B) the cell entered and completed a normal anaphase (not depicted). Although the duration of prometaphase in these cells was highly variable, it was usually significantly longer (up to 60 min) than in those cells in which NEB occurred in the presence of completely separated centrosomes.

The kinetochore-directed formation of K-fibers also occurred on mono-oriented chromosomes positioned close to one of the spindle poles (Fig. 2). As described above, K-fibers were seen to grow out of the kinetochore that was shielded from the proximal centrosome by the chromosome body. Remarkably, the initial orientation of the growing K-fiber was not toward the distal centrosome, as would be predicted if fiber formation was initiated by the capture of an astral MT. Instead, forming K-fibers initially extended toward the cell's periphery. At some point in time they then exhibited a sudden turn, and their free ends began to migrate toward a centrosome as if they were captured by astral MTs. On occasion it was possible to detect astral MTs that approached a growing K-fiber just before it initiated motion toward a centrosome (i.e., toward a pole; Fig. 2). Importantly, the formation of this distal K-fiber, and its subsequent movement toward a spindle pole, transported the chromosome to the spindle equator (Fig. 2; Savoian and Rieder, 2002). The features of this motion were similar to congression motions that occur after an unattached kinetochore on a mono-oriented chromosome is captured by an astral MT (Skibbens et al., 1993; Khodjakov et al., 1997).

Thus far, our data reveal that kinetochores in S2 cells can form K-fibers by a centrosome-independent mechanism. Does this kinetochore-driven K-fiber formation also occur on kinetochores that are oriented toward a centrosome? This question is difficult to address because in most cells the astral MT density makes it impossible to clearly follow how the kinetochore acquires its MTs. However, in highly flattened cells the density of astral MTs in the vicinity of the chromosomes is significantly decreased. This, in turn, decreases the chances of astral MT capture which allowed us to follow the formation of indi-

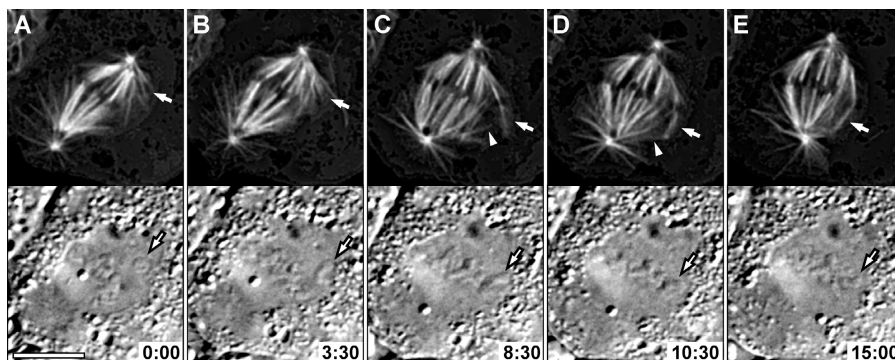
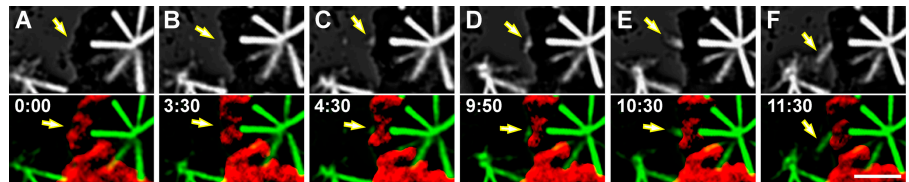


Figure 2. Formation of a K-fiber on the distal kinetochore of a mono-oriented chromosome leads to chromosome congression. (A–E) Selected frames from a combinational fluorescence (top)/DIC (bottom) time-lapse sequence. This cell contains a mono-oriented chromosome (A, bottom, arrow), which is positioned near the top spindle pole. A K-fiber forms in association with the unattached kinetochore that faces away from centrosome-generated astral MTs (top, arrows). This fiber initially grows from the kinetochore toward the cell's periphery (B and C), but it then suddenly turns toward the bottom spindle pole and begins to glide poleward (compare C with D). As the result of the gliding, the fiber becomes incorporated into the spindle, and the chromosome congresses onto the metaphase plate (E). Note that poleward sliding of the fiber is initiated when it interacts with an astral MT emanating from the bottom pole (arrowheads in C and D). Time is in min:s. Bar, 5 μ m.

porated into the spindle, and the chromosome congresses onto the metaphase plate (E). Note that poleward sliding of the fiber is initiated when it interacts with an astral MT emanating from the bottom pole (arrowheads in C and D). Time is in min:s. Bar, 5 μ m.

Figure 3. MT initiation from kinetochores in the presence of centrosomes. (A–F) Selected frames from a combinational fluorescence/DIC time-lapse recording. Top part of each frame presents deconvolved and contrast-EGFP/ α -tubulin fluorescence, whereas the bottom part of each frame is an overlay of fluorescence (green) over chromosome contours (red) from the corresponding DIC images. The cell is met with a mono-oriented chromosome, which is connected to one spindle pole via well-developed K-fiber, whereas the second kinetochore on this chromosome is completely devoid of MTs (A). This kinetochore remains unattached for several minutes (B). Then, however, formation of a small but discrete patch of GFP/ α -tubulin fluorescence is seen in association with this kinetochore (C). The intensity of the patch gradually increases and eventually it begins to elongate forming a K-fiber (D–F). Note that the growing fiber is initially oriented away from the centrosome (E) but it then suddenly turns and becomes oriented toward the centrosome. Time is in min:s. Bar, 5 μ m.



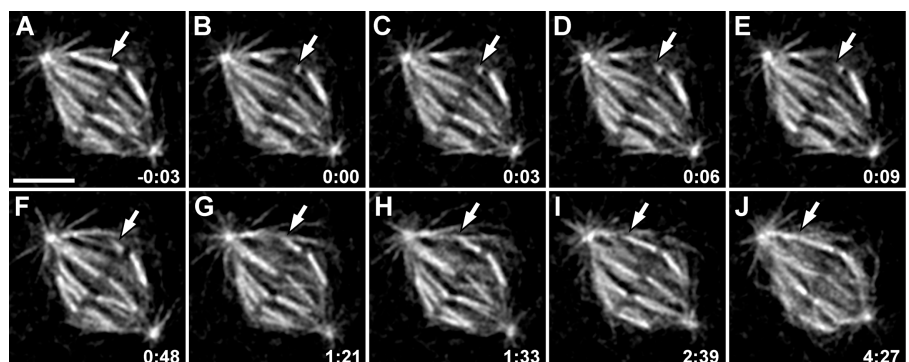
vidual K-fibers on kinetochores that were oriented toward a centrosome. In these cells kinetochores remain free of MTs for several minutes (Fig. 3, A and B). At the end of this time a weak GFP signal, likely corresponding to several short MTs, appeared in the kinetochore region (Fig. 3, C and D). Soon thereafter, an MT bundle began to extend from the kinetochore outwards (Fig. 3, E and F). Because the initial growth direction of these forming MT bundles was not toward a centrosome (Fig. 3 E) they were not connected to a centrosome and thus could not have been formed via the classic search-and-capture mechanism. In the example shown in Fig. 3, the growing fiber exhibits a sudden turn, after which its free end orients toward a centrosome as it captures and is transported poleward on astral MTs (Fig. 3 F).

Growth of K-fibers occurs by MT subunit addition at the kinetochore

Our finding that some K-fibers grow from the kinetochores in S2 cells raises the important question of where tubulin subunits added to the forming K-fiber? MTs in K-fibers are organized in a parallel bundle with their minus ends terminating near the spindle pole and their plus ends ending within the kinetochore. In a mature K-fiber, tubulin heterodimers are constantly added in the kinetochore, and removed from the minus ends in the pole. As a result, even when the length of the fiber remains constant the subunits “flux” poleward through the fiber (Mitchison, 1989). Importantly, flux requires that MT plus- and minus-end dynamics within the K-fiber be precisely coordinated, so that during metaphase the length of the fiber

remains constant. Obviously, during K-fiber growth from the kinetochore, the rate of MT polymerization must exceed the depolymerization rate. This implies that either the minus-end depolymerization is suppressed or that plus-end polymerization rate is increased in K-fibers before they connect to the pole. To differentiate between these two possibilities we severed individual K-fibers within the spindle with a focused laser beam and then followed them by fluorescence time-lapse microscopy (Fig. 4 and Video 4, available at <http://www.jcb.org/cgi/content/full/jcb.200407090/DC1>). Severing a K-fiber results in the formation of two fragments: one (the P-fragment) remains connected to the spindle pole by its MT minus ends, and it now has (new) free MT plus ends; the other (K-fragment) remains connected to the kinetochore via its MT plus ends, whereas its newly created MT minus ends are free. In agreement with similar K-fiber severing experiments of others (Inoue, 1964; Forer, 1965; Spurck et al., 1990; Czaban et al., 1993; Forer et al., 1997), we find that the behaviors of these fragments are strikingly different. In all cases ($n = 15$) P-fragments shorten rapidly and completely disappear in <10 s (Fig. 4, A–E). In contrast, K-fragments remain stable and then regrow (Fig. 5 A) to the length of the original K-fiber (Fig. 4, B–J). In five of these cells we were able to measure the shrinkage and regrowth rates, which were $21.8 \pm 0.4 \mu\text{m}/\text{min}$ and $0.8 \pm 0.2 \mu\text{m}/\text{min}$, respectively. Notably, as the K-fragments begin to elongate they need not be oriented toward a centrosome (Fig. 4, F and G), but at some point the elongating MT bundle turns so that its minus end becomes oriented toward a centrosome, and growth then con-

Figure 4. Severed K-fibers regrow from the kinetochore. (A–J) Selected frames from a fluorescence time-lapse recording. An individual K-fiber is severed by a laser microbeam (compare arrows in A and B). This operation creates two K-fiber fragments: one fragment remains associated with the spindle pole and has free plus ends (P-fragment) and the other fragment remains associated with the kinetochore and now has free minus ends (K-fragment). The P-fragment rapidly depolymerizes toward the pole within the first 10 s after cutting (B–E). In contrast, the K-fragment regrows back to its original length (B–J). Initially, the regrowing fragment is not oriented toward the spindle pole (D–G). Later, however, it turns and becomes incorporated into the spindle (H–J). Time is in min:s. Bar, 5 μ m.



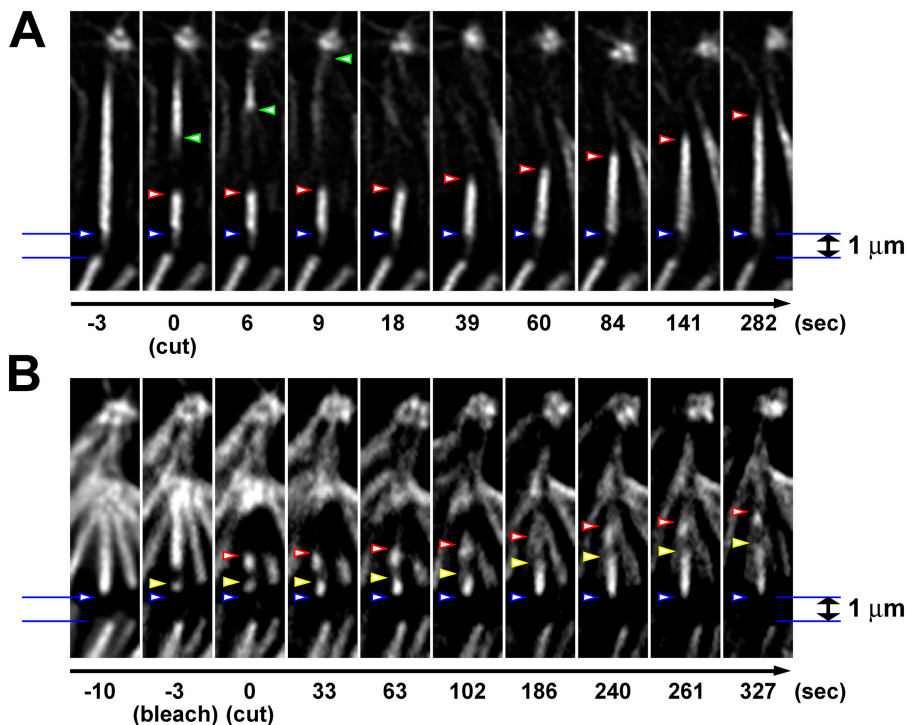


Figure 5. K-fibers regrow by MT plus-end polymerization after laser microsurgery. (A) Selected frames from fluorescence time-lapse recording depicting the behavior of K-fiber fragments generated by laser microsurgery. Note that the pole-connected fragment (P-fragment) rapidly depolymerizes, whereas the kinetochore-attached fragment (K-fragment) grows steadily. Green arrowheads point to the position of the free end of P-fragment, whereas red arrowheads mark the position of the K-fragment's free end. Blue arrowheads point at the end of the K-fiber terminating in the kinetochore. (B) Selected frames from a fluorescence time-lapse sequence of a combinational laser microsurgery/photobleaching experiment. In this cell, a short segment of an individual K-fiber is first photobleached with a low power 488-nm laser (compare -10 with -3 s frames). Then, the same fiber is cut with high power 532-nm laser pulses in the region immediately outside the bleached segment (compare -3 and 0 s frames). As the result, the K-fragment created by the operation now contains a fiduciary mark that allows us to determine where the elongation of the fragment is occurring via subunit incorporation into the kinetochore-associated (plus) or free (minus) ends of MTs. Red arrowheads indicate the position of the fragment's free end, whereas yellow arrowheads point at the bleached

segment. Blue arrowheads point at the end of the K-fiber terminating in the kinetochore. As is evident from the preservation of the distance between the bleached segment and the free end of the fragment, elongation occurs via plus-end MT polymerization (in the kinetochore). It also reveals that the minus ends of MTs are stable under our conditions.

tinues until the minus end reaches the spindle pole (Fig. 4, H–J). Thus, K-fragments exhibit both features of kinetochore-driven K-fiber formation: they elongate from the kinetochore toward the cell periphery, irrespective of the position of the centrosomes, and free ends are eventually captured and directed toward a centrosome (spindle pole) by astral MTs.

Intriguingly, severing one of the two sister K-fibers on bi-oriented chromosomes had no effect on the position of the chromosome. A chromosome positioned on the spindle equator did not move even when one of its K-fibers was severed very near the kinetochore (15 operations), generating a stub as short as $1 \mu\text{m}$ (Fig. 5 and Video 5, available at <http://www.jcb.org/cgi/content/full/jcb.200407090/DC1>). Furthermore, the distance between the plus ends of the sister K-fibers did not change after one of the fibers was severed, or as it regrew and reconnected to the pole. These results indicate that the tension across the centromere does not change when the K-fibers are not anchored at spindle poles. This is somewhat unexpected considering that interkinetochore distances in *Drosophila* S2 cells are reported to decrease upon taxol treatment (Logarinho et al., 2004; Fig. S1, available at <http://www.jcb.org/cgi/content/full/jcb.200407090/DC1>), which implies the existence of tension across the centromere in S2 cells during metaphase. Furthermore, when we split centromeres between sister kinetochores apart with the laser beam during metaphase, each kinetochore moved toward its attached pole (not depicted; Savoian et al., 2000). This observation reveals the existence of a poleward pulling force throughout metaphase that acts along the K-fiber. Our data implies that the magnitude of this force is the same, so that the chromosome remains stationary on the spin-

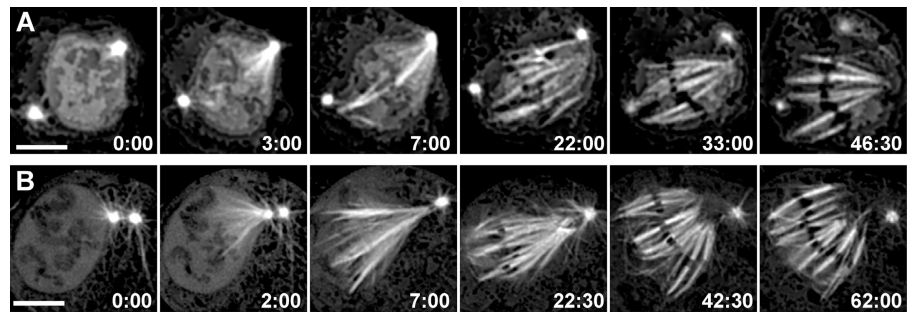
dle equator, whether it acts on a $1\text{-}\mu\text{m}$ stub or on a fully grown $5\text{--}7\text{-}\mu\text{m}$ -long K-fiber.

The rate at which K-fragments elongate is equivalent to the rate of poleward flux in S2 cells ($0.7 \pm 0.2 \mu\text{m}/\text{min}$; unpublished data). To determine if K-fragment elongation occurs from tubulin subunit addition at kinetochore MT plus, or minus ends we combined laser microsurgery with photobleaching. In these experiments we first photobleached a K-fiber segment adjacent to the kinetochore, and then severed the same fiber just outside the bleached region toward the pole. Time-lapse microscopy reveals that the distance between the bleached segment and the free end of the fragment does not change during fragment elongation (Fig. 5 B). Thus, the new MT minus ends created by severing a K-fiber are stable. By contrast, the distance between the bleached segment and the kinetochore increases as the fragment elongates, and this increase accounts for the total amount of fragment growth. This result clearly reveals that K-fragment elongation occurs via the incorporation of new tubulin subunits into MT plus ends within the kinetochore.

Inhibiting cytoplasmic dynein does not affect kinetochore-driven K-fiber formation but it prevents their integration into a common spindle pole

An interesting feature of kinetochore-driven K-fiber formation in S2 cells is that growing (or regrowing) K-fibers are initially oriented randomly relative to the centrosomes. At some point, however, the free (minus) end of the fibers invariably turn and become oriented toward a centrosome, as if they are captured by and transported along an astral MT. Previous studies sug-

Figure 6. Spindle assembly in dynein-depleted cells. Selected frames from fluorescence time-lapse sequences of cells undergoing mitosis ~ 72 h after dynein RNAi. (A) Spindle formation in a cell with centrosomes completely separated before NEB. The spindle forms between the separated centrosomes, and the poles are initially well focused. However, at a later time, the centrosomes detach from the poles and the K-fibers splay so that the spindle becomes barrel shaped. (B) Spindle formation in a cell with non-separated centrosomes, and the poles are initially well focused. Under this condition, the spindle initially forms as a fan-shaped structure, with MTs converging on the centrosome(s) only on one side of the chromosomes (2:00). However, within just a few minutes formation of prominent K-fibers is seen on the other side of the chromosomes (7:00). These K-fibers do not converge on a common point. Over time, the centrosomes detach from the spindle and then the K-fibers on the side of the spindle that was initially well focused begin to splay. As a result, the spindle eventually becomes barrel-shaped (62:00). Note that in this cell the centrosomes fused together (between 2:00 and 7:00), so that they appear as a single structure in later frames. Bars, 5 μ m.



gested that NuMA, which localizes to the free MT minus ends of K-fibers forming from kinetochores in monastrol-treated cells (Khodjakov et al., 2003), is responsible for K-fiber incorporation into the spindle. Although NuMA itself does not possess motor activity, it is known to be part of the dynein–dynactin complex (Merdes et al., 1996; Gaglio et al., 1997). These observations suggest that the capture and transport of preformed K-fibers in S2 cells is mediated by dynein. To test this we followed the formation of spindles in S2 cells depleted of cytoplasmic dynein by RNAi (Fig. S2, available at <http://www.jcb.org/cgi/content/full/jcb.200407090/DC1>).

As reported by others, dynein knockdown induces S2 cells to accumulate in mitosis (Goshima and Vale, 2003; Fig. S2). In most of these cells the spindles were roughly bipolar and the chromosomes were organized into loose metaphase plates. However, compared with controls, under the experimental conditions we used, the poles were conspicuously less focused so that the spindle appeared barrel-shaped as in plants. Often the centrosomes were displaced from the spindle poles (Fig. 6 A), or had failed to separate (Fig. 6 B). These phenotypes are generally consistent with the effects of dynein inhibition reported previously in *Drosophila* (Robinson et al., 1999) and mammalian cells (Echeverri et al., 1996).

Time-lapse microscopy revealed that spindle formation in dynein-depleted cells occurs by two distinct pathways. In cells where the centrosomes were well separated at NEB, the spindle formed between the centrosomes (Fig. 6 A and Video 6, available at <http://www.jcb.org/cgi/content/full/jcb.200407090/DC1>). Under this condition, prominent K-fibers that were focused on the centrosomes formed during the first ~ 15 min after NEB. With time, however, the centrosomes usually became detached from the spindle poles and wandered away (Fig. 6 A). When this happened the K-fibers remained stable but their minus ends began to separate until the poles lacked focus. The level of convergence could be dramatically different between opposing half-spindles so that, in extreme cases, the spindle became fan-shaped (Fig. 6 A). In most cases, however, the splaying was less dramatic and produced a barrel-shaped spindle (Fig. S2).

In those cells where the centrosomes were unseparated at NEB, astral MTs penetrated just one side of the region occu-

ried by the former nucleus. As they did so a monopolar spindle began to form on the side of the chromosomes that faced the centrosomes (Fig. 6 B and Video 7). However, within 15 min K-fibers also began to form on the distal kinetochores that faced away from the centrosomes. These K-fibers grew away from the chromosomes and failed to converge on a common focus (Fig. 6 B). As a result, the spindle in these cells appeared fan-shaped with K-fibers focusing on the centrosome in one half-spindle, and diverging or oriented parallel to each other in the other half-spindle. Over time, the centrosomes in these cells also detached from the spindles, which led the K-fibers to splay and form a barrel-shaped spindle (Fig. 6 B).

Discussion

Mitotic spindle assembly requires two major activities. First, MT nucleation and growth must be promoted. Second, these MTs must then be sorted into a single bipolar structure so that their plus ends are oriented toward the chromosomes and their minus ends toward a common pole. It is generally assumed that in higher animal cells centrosomes are responsible for both these activities. This assumption has, however, been challenged by the recent finding that an alternative centrosome-independent pathway that promotes MT nucleation and “self-organization” during mitosis exists, even in those cells that normally contain centrosomes (for review see Wadsworth and Khodjakov, 2004).

Kinetochores can initiate K-fiber formation during mitosis in animals

Our data reveal that K-fibers formed consistently on those kinetochores that were shielded from, and thus could not capture, centrosome-generated astral MTs. Furthermore, in some cases we were able to follow the initiation of K-fiber formation (Fig. 3), thus demonstrating directly that fiber formation starts in the vicinity of the kinetochore. These observations raise the question of whether kinetochores can nucleate MTs.

There are reports that kinetochores on isolated chromosomes (Telzer et al., 1975) and in lysed mitotic cells (Snyder and McIntosh, 1975; Gould and Borisy, 1978) act as initiating sites for MT polymerization when incubated with purified tu-

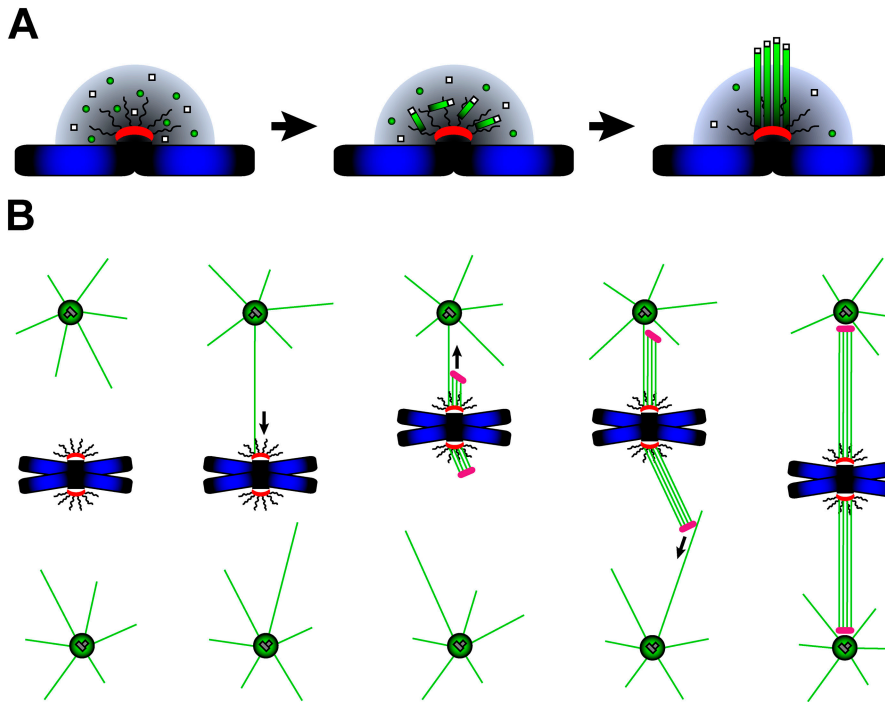


Figure 7. Model for initiation of K-fiber formation by kinetochores during normal spindle formation. (A) Chromosomes/centromeres provide a favorable environment for MT nucleation, e.g., by generating a RanGTP gradient (green circles represent α/β -tubulin heterodimers, and white squares represent a putative initiation factor). This leads to formation of short MTs in the vicinity of kinetochores, where these MTs can be easily captured. When an MT is captured by its plus end, it begins to polymerize steadily within the kinetochore. As the result, MT minus ends are pushed away from the kinetochores. Additional factors are likely responsible for cross-linking individual MTs to form a K-fiber. (B) Two routes leading to K-fiber formation and spindle morphogenesis. When unattached kinetochores capture astral MTs (top kinetochore in the schematics) they immediately establish a connection to the pole and move poleward. Then, a mature K-fiber can form either by acquiring additional astral MTs or through kinetochore-mediated MT polymerization (shown). Importantly, in this scenario the growth of the K-fiber from the kinetochore will be directed to the attached pole. An alternative route of K-fiber formation (bottom kinetochore in the schematics) is used when the connection between the kinetochore and the pole is delayed (e.g., kinetochores facing

away from the pole). Under this condition, the kinetochores themselves initiate formation of K-fibers, via the mechanism presented in A. The initial growth of these K-fibers is not directed toward spindle poles, but eventually the minus ends of growing K-fibers interact with astral MTs and are subsequently incorporated into the spindle.

bulin. Furthermore, EM analyses revealed formation of short MTs in the vicinity of the kinetochores in cells recovering from MT poisons (Witt et al., 1980; De Brabander et al., 1981). These short MTs were first seen in the area around the kinetochores, and only later became attached to the kinetochore plate proper. Importantly, MTs were more likely to form in the vicinity of kinetochore clusters than in association with individual kinetochores (Witt et al., 1980).

Despite the early data that kinetochores can induce the assembly of MTs, the idea that this activity contributes to K-fiber formation during a normal animal mitosis has been largely ignored. The major reason for that was that if kinetochores nucleate MTs via a standard template mechanism involving, e.g., γ -tubulin rings anchored to the kinetochore (for review see Yu et al., 2000), then the minus ends of each MT would be attached to the kinetochore, whereas the plus ends would point away from the chromosome. However, K-fiber MTs are known to have the same polarity as astral MTs, even in cells recovering from a colcemid block (Euteneuer and McIntosh, 1981; Euteneuer et al., 1983). Furthermore, our data reveal that the elongation of K-fibers generated by kinetochores occurs via the incorporation of tubulin subunits into MT plus ends at the kinetochore, whereas the minus ends pointing away from chromosomes remain stable (Fig. 5). Thus, it is conceptually difficult to understand how MTs nucleated by the kinetochore would form a K-fiber with proper polarity (MT minus ends toward the pole).

However, our observations combined with demonstrations that MT nucleation is stimulated in the vicinity of centrosomes, offer a straightforward explanation for how kineto-

chores can generate K-fibers with the correct polarity (Fig. 7 A). We believe that kinetochores do not nucleate but rather capture short MTs that form in their vicinity as described by Witt and colleagues (Witt et al., 1980). Nucleation of these short MTs is likely to be promoted by a Ran-GTP gradient (for review see Karsenti and Vernos, 2001), although we have yet no experimental proof for this hypothesis. It has been shown, however, that RCC1 (the GTP exchange factor for Ran) is concentrated in the centromere (Bischoff et al., 1990). In fact, RCC1 was independently identified as the centromere-associated protein CENP-D (Kingwell and Rattner, 1987). Furthermore, other proteins involved in the Ran GTP/GDP cycle are also enriched in the centromere/kinetochore region (Joseph et al., 2004). Thus, it is likely that the favorable environment in the vicinity of kinetochores promotes MT nucleation.

Centrosomes collect the ends of K-fibers into spindle poles via a dynein-dependent mechanism

Our data reveal that an individual kinetochore is sufficient to form an associated K-fiber. One consequence of this is that each chromosome should be able to build a "mini-spindle" consisting of just two K-fibers emanating from its sister kinetochores. In fact, the existence of such mini-spindles has been demonstrated in vertebrate somatic cells after inhibition of the activities of the proteins responsible for spindle-pole organization (Gordon et al., 2001). Normally, however, the mitotic spindle in animals forms as an integrated structure in which all K-fibers in each half-spindle converge on a common centrosome-associated pole.

Our observations reveal that when a kinetochore forms a K-fiber it is rarely initially oriented toward a spindle pole (centrosome). Instead, the forming fiber grows away from the kinetochore regardless of the direction in which the kinetochore faces. Then, at some point, the distal end of the growing fiber exhibits a sharp turn, and moves into a centrosome (Figs. 2 and 3). The most straightforward explanation for the sudden change in K-fiber orientation is that it encounters and attaches to one or more astral MTs that then direct its motion toward the centrosome. This incorporation of individual K-fibers into the common spindle does not occur after inhibiting cytoplasmic dynein by RNAi (Fig. 6 and Fig. S2). Our results also demonstrate that dynein activity is not required for K-fiber formation proper which contradicts the claim that dynein is required for bringing MTs to the attachment sites (Rogers et al., 2004).

Thus, astral MTs search for and capture more than unattached kinetochores. Rather, they are responsible for transporting poleward multiple preassembled spindle components, including K-fibers, and integrating them into a common structure.

The coexistence of centrosome- and kinetochore-driven K-fiber formation

Our data reveal that the formation of K-fibers in animal cells, and their incorporation into the spindle, occurs in any given cell via two distinct routes (Fig. 7 B). By chance, some kinetochores directly interact with astral MTs, whereas others, shielded from such an interaction, remain devoid of MTs. The astral MT–kinetochore interaction results in the attachment of the kinetochore to the pole, which is initially mediated by one or just a few MTs, and it is then somehow transformed into a well-developed K-fiber containing 15–30 MTs. The continued accumulation of MTs by the kinetochore is viewed to occur via the repetitive capture of additional astral MTs (McEwen et al., 1997). However, the data presented here raise the possibility that the growth of kinetochore-generated MTs can also contribute to the maturation of K-fibers (Fig. 7 B).

A chromosome that cannot interact with an astral MT (e.g., due to spatial constraints) will remain motionless. As the result, over time factors that promote MT nucleation (e.g., RanGTP) will become enriched around centromeres of these chromosomes. In turn, a local enrichment induces the formation of numerous short MTs in the vicinity of the kinetochore, which are then captured to initiate K-fiber formation. During capture, MT plus ends become embedded in the kinetochore plate, after which they begin to incorporate additional MT subunits. This growth then pushes the MT minus end away from the kinetochore. The minus ends of MTs within K-fibers appear to be stable (Fig. 5). This feature is not unexpected as it was suggested from previous K-fiber—cutting experiments (Wilson and Forer, 1989; Spurck et al., 1990; Czaban et al., 1993), although it was never experimentally verified. Thus, stability of the minus ends is likely an intrinsic property of kinetochore MTs. It also implies that factors responsible for MT subunit flux, which requires the removal of tubulin subunits from the minus ends of K-fiber MTs, are concentrated in the polar regions during metaphase (Rogers et al., 2004).

The elongation of kinetochore-organized K-fibers increases their probability of being captured by astral MTs. Consequently, over time each growing K-fiber is captured and its minus end is transported poleward via a dynein dependent process. Remarkably, the incorporation of kinetochore-organized K-fibers into the spindle results in congression of the attached chromosome (Fig. 2 and Fig. 7 B; Savoian and Rieder, 2002). Thus, the incorporation and transport of preformed K-fibers provides an alternative mechanism for achieving proper chromosome orientation and positioning during mitosis in animals.

Kinetochore and K-fiber dynamics during metaphase

When a chromosome becomes bi-oriented the distance between its sister kinetochores increases (for review see Rieder and Salmon, 1998), because the centromere is now experiencing tension generated by poleward forces acting along the K-fibers. The origin of these forces appears to vary in different cell types, as does the behavior of the kinetochores. In vertebrate somatic cells, an attached kinetochore repeatedly switches (oscillates) between periods of active poleward movement, which is coupled to plus-end depolymerization of K-fiber MTs (P-state), and away-from-the-pole movement, which is coupled to plus-end polymerization (N-state). During P-state kinetochores exert an active pulling force on the centromere (for review see Rieder and Salmon, 1998). During N-state they resist away-from-the-pole motions, acting as a “slip-clutch” (Maddox et al., 2003). At any given time in vertebrates, one of the sister kinetochores is trying to move poleward, whereas its sister resists this motion, or attempts to actively move in the opposite direction. This tug-of-war produces tension across the centromere, which is manifested as a stretching.

The situation is, however, different in systems where kinetochores do not oscillate, including, e.g., plants, *Xenopus* egg extracts, and *Drosophila* and other insect cells. In these systems, both sister kinetochores are locked in a persistent N-state (Maddox et al., 2003; Chen and Zhang, 2004) that does not actively produce tension across the centromere. Instead, tension has been proposed to be generated by the poleward movement (flux) of MT subunits within the opposing K-fibers (Inoue and Salmon, 1995; Kapoor and Compton, 2002). Our data are inconsistent with this hypothesis. We find that severing one K-fiber on a metaphase chromosome close to the kinetochore does not decrease the distance between the sister kinetochores, nor does it induce a change in the chromosome position. The former observation reveals that the centromere remains under tension. However, this tension cannot be produced by flux, as the fiber is disconnected from the pole. Furthermore, the lack of chromosome repositioning after severing one of the sister K-fibers reveals that the magnitude of the force acting on the sister kinetochores is not proportional to the length of the fiber. This observation eliminates traction-fiber mechanisms in force generation (Maddox et al., 2003).

Finally, we found that when K-fibers were severed during metaphase in S2 cells, they regrew to their normal length by MT subunit addition at the kinetochore. During this growth the newly formed MT minus ends remain stable. Using similar

methods, Chen and Zhang (2004) found that minus ends of K-fiber MTs, generated by severing K-fibers in grasshopper spermatocytes during anaphase, continuously lose tubulin subunits even when the fiber is not connected to the spindle pole. However, during this time the length of the fiber remains constant because MT subunits are also added into the MT plus ends at the same rate they are removed from the minus ends (i.e., MT subunits “treadmill” away from the kinetochore; Chen and Zhang, 2004). Because our results and those of Chen and Zhang (2004) were obtained in similar systems, they likely reflect a real change in K-fiber dynamics at anaphase onset. If true, it means that the metaphase-anaphase transition has a greater effect on the stability of MT minus ends than on the functional state of kinetochores. Clearly, this is an important area for further exploration.

Materials and methods

Cell culture

All experiments reported here were conducted on *Drosophila* S2 cells that stably express GFP/ α -tubulin (S2T); cells were cultured as described previously (Goshima and Vale, 2003). The level of tubulin overexpression in these cells is ~20% (Fig. S3, available at <http://www.jcb.org/cgi/content/full/jcb.200407090/DC1>).

Flattening of S2 cells for live microscopy studies

Microscopy analyses of dividing *Drosophila* S2T cells were conducted as described previously (Fleming and Rieder, 2003) with modifications. In brief, a drop of medium containing exponentially growing cells was placed on an uncoated coverslip for 10 min. An $\sim 5 \times 5 \times 0.5$ -mm piece of agarose was gently put on top of the cells. The coverslip was then flipped and placed onto two different thickness spacers resting on a glass slide. As the result cells closer to the thicker spacer remained relatively rounded, whereas cells on the other side of the coverslip became extremely flat. This approach allowed us to create a gradient of flatness and then select those cells that were ideal for high resolution LM analyses, but were not inhibited in their mitotic progression or cytokinesis. The edges of the coverslip were then sealed with VALAP (1:1:1 vaseline/lanolin/paraffin) to prevent evaporation.

RNAi and time-lapse light microscopy analyses

The depletion of cytoplasmic dynein heavy chain from *Drosophila* S2T cells by RNAi was performed according to previously published protocols (Maiato et al., 2003) using specific primers to target a sequence of 700 bp (forward primer: AGTAGCCCGAGGAATGATCC; reverse primer: CCATGGGGAGCTAAGTGG). Live cell analyses were performed 3 d after the addition of dsRNA into cultures, when dynein had been totally depleted, as confirmed by Western blot analysis. Image series were collected every 30 s or every 3 s in the case of laser microsurgery at 24–26°C using either an Olympus IX70 or a Nikon Eclipse TE2000E DIC inverted light microscope. These were equipped, respectively, with a CM350 or CoolSnap HQ camera (Photometrics), and time-lapse datasets were subsequently deblurred using the deconvolution algorithm from SoftWorx 2.5 (Applied Precision). Image sequences were compiled with ImageJ 1.30 (NIH). Contrast was adjusted using Photoshop 6.0 (Adobe Systems).

Laser microsurgery and photobleaching

Laser microsurgery was conducted on a custom-assembled workstation centered around a microscope (model TE2000E; Nikon Instruments). We used an independent second (lower) epi-port that is available on this model, to steer collimated laser beams into to the back aperture of a 60 \times A 1.4-NA PlanApo lens. As a result, both the 532-nm beam used for laser cutting (Nd:YAG laser; 7-ns pulses, 10 Hz) and the 488-nm continuous wave beam used for photobleaching (Argon-ion laser; 15 mW), were focused to a diffraction-limited spot in the object plane. The beams were steered with custom-made dichroic mirrors (Chroma Technology Corp.) that resided in the lower filter-cube turret. The top turret contained a standard “Endow” filter cube for imaging GFP fluorescence (Chroma Technology Corp.). This turret was motorized so that the imaging cube could be temporarily moved out of the optical path during photobleaching routines.

Because the laser pulses used for microsurgery were longer in wavelength than was the GFP emission, it was not necessary to remove the GFP imaging cube from the optical path during laser microsurgery. This arrangement allows us to achieve high efficiency fluorescence while avoiding any lateral shifts in the position of the cutting beam, as is usually associated with switching between different dichroic mirrors. Furthermore, we were able to observe the effects of laser microsurgery immediately after the operation.

All light sources in our system were shuttered with fast UniBlitz shutters (Vincent Associates), so that each cell was exposed to light only during laser operations and/or image acquisition. The whole system was driven by IP Lab software (Scanalytics) run on a PC.

Online supplemental material

Fig. S1 shows that taxol treatment decreases distances between sister kinetochores in *Drosophila* S2 cells. Fig. S2 depicts depletion efficiency and mitotic characterization after dynein RNAi. Fig. S3 depicts quantification of the total α -tubulin levels present in the stable cell line expressing GFP/ α -tubulin. Video 1 corresponds to images presented in Fig. 1 A. Video 2 corresponds to images presented in Fig. 1 B. Video 3 corresponds to images presented in Fig. 2. Video 4 corresponds to images presented in Fig. 4. Video 5 corresponds to images presented in Fig. 5 A. Video 6 corresponds to images in Fig. 6 B. Video 7 is another example of splaying of K-fibers upon centrosome detachment in dynein-depleted cells. Online supplemental material is available at <http://www.jcb.org/cgi/content/full/jcb.200407090/DC1>.

We thank Drs. Ron Vale (University of San Francisco, San Francisco, CA), Tom Hays (University of Minnesota, Minneapolis, MN), Claudio Sunkel (University of Porto, Porto, Portugal), and Gary Karpen (University of California at Berkeley, Berkeley, CA) for providing reagents.

This work was supported by National Institutes of Health grants GM59363 (to A. Khodjakov) and GM40198 (to C. Rieder). H. Maiato is the recipient of postdoctoral research fellowship SFRH/BPD/11592/2002 from Fundação para a Ciência e a Tecnologia of Portugal. Construction of the laser microsurgery system was supported in part by a Nikon/Marine Biological Laboratory fellowship (to A. Khodjakov).

Submitted: 15 July 2004

Accepted: 29 October 2004

References

- Bajer, A.S. 1987. Substructure of the kinetochore and reorganization of kinetochore microtubules during early prometaphase in *Haemaphysalis* endosperm. *Eur. J. Cell Biol.* 43:23–34.
- Bischoff, F.R., G. Maier, G. Tilz, and H. Ponstingl. 1990. A 47-kDa human nuclear protein recognized by antikinetochore autoimmune sera is homologous with the protein encoded by RCC1, a gene implicated in onset of chromosome condensation. *Proc. Natl. Acad. Sci. USA.* 87:8617–8621.
- Bonaccorsi, S., M.G. Giansanti, and M. Gatti. 1998. Spindle self-organization and cytokinesis during male meiosis in asterless mutants of *Drosophila melanogaster*. *J. Cell Biol.* 142:751–761.
- Chen, W., and D. Zhang. 2004. Kinetochore fibre dynamics outside the context of the spindle during anaphase. *Nat. Cell Biol.* 6:227–231.
- Czaban, B.B., and A. Forer. 1985. The kinetic polarities of spindle microtubules in vivo, in crane-fly spermatocytes. I. Kinetochore microtubules that reform after treatment with colcemid. *J. Cell Sci.* 79:1–37.
- Czaban, B.B., A. Forer, and A.S. Bajer. 1993. Ultraviolet microbeam irradiation of chromosomal spindle fibres in *Haemaphysalis katherinae* endosperm. I. Behaviour of the irradiated region. *J. Cell Sci.* 105:571–578.
- De Brabander, M., G. Geuens, J. De May, and M. Joniau. 1981. Nucleated assembly of mitotic microtubules in living PTK2 cells after release from nocodazole treatment. *Cell Motil.* 1:469–483.
- Echeverri, C.J., B.M. Paschal, K.T. Vaughan, and R.B. Vale. 1996. Molecular characterization of the 50-kD subunit of dynactin reveals function for the complex in chromosome alignment and spindle organization during mitosis. *J. Cell Biol.* 132:617–633.
- Euteneuer, U., and J.R. McIntosh. 1981. Structural polarity of kinetochore microtubules in PtK1 cells. *J. Cell Biol.* 89:338–345.
- Euteneuer, U., H. Ris, and G.G. Borisy. 1983. Polarity of kinetochore microtubules in Chinese hamster ovary cells after recovery from a colcemid block. *J. Cell Biol.* 97:202–208.
- Fleming, S., and C.L. Rieder. 2003. Flattening *Drosophila* cells for high-resolution light microscopic studies of mitosis in vitro. *Cell Motil. Cytoskele-*

ton. 56:141–146.

- Forer, A. 1965. Local reduction of spindle fiber birefringence in living *Nephrotoma Suturalis* (Loew) spermatocytes induced by ultraviolet microbeam irradiation. *J. Cell Biol.* 25:95–117.
- Forer, A., T. Spurck, and J.D. Pickett-Heaps. 1997. Ultraviolet microbeam irradiations of spindle fibres in crane-fly spermatocytes and newt epithelial cells: resolution of previously conflicting observations. *Protoplasma.* 197:230–240.
- Gaglio, T., M.A. Dionne, and D.A. Compton. 1997. Mitotic spindle poles are organized by structural and motor proteins in addition to centrosomes. *J. Cell Biol.* 138:1055–1066.
- Gordon, M.B., L. Howard, and D.A. Compton. 2001. Chromosome movement in mitosis requires microtubule anchorage at spindle poles. *J. Cell Biol.* 152:425–434.
- Goshima, G., and R.D. Vale. 2003. The roles of microtubule-based motor proteins in mitosis: comprehensive RNAi analysis in the *Drosophila* S2 cell line. *J. Cell Biol.* 162:1003–1016.
- Gould, R.R., and G.G. Borisy. 1978. Quantitative initiation of microtubule assembly by chromosomes from Chinese hamster ovary cells. *Exp. Cell Res.* 113:369–374.
- Hayden, J.H., S.S. Bowser, and C.L. Rieder. 1990. Kinetochores capture astral microtubules during chromosome attachment to the mitotic spindle: direct visualization in live newt lung cells. *J. Cell Biol.* 111:1039–1045.
- Hinchcliffe, E.H., F.J. Miller, M. Cham, A. Khodjakov, and G. Sluder. 2001. Requirement of a centrosomal activity for cell cycle progression through G₁ into S phase. *Science.* 291:1547–1550.
- Inoue, S. 1964. Organization and function of the mitotic spindle. In *Primitive Motile Systems in Cell Biology*. R.D. Allen and N. Kamiya, editors. Academic Press, New York, London. 549–598.
- Inoue, S., and E.D. Salmon. 1995. Force generation by microtubule assembly/disassembly in mitosis and related movements. *Mol. Biol. Cell.* 6:1619–1640.
- Joseph, J., S.T. Liu, S.A. Jablonski, T.J. Yen, and M. Dasso. 2004. The RanGAP1-RanBP2 complex is essential for microtubule-kinetochore interactions in vivo. *Curr. Biol.* 14:611–617.
- Kapoor, T.M., and D.A. Compton. 2002. Searching for the middle ground: mechanisms of chromosome alignment during mitosis. *J. Cell Biol.* 157:551–556.
- Karsenti, E., and I. Vernos. 2001. The mitotic spindle: a self-made machine. *Science.* 294:543–547.
- Khodjakov, A., R.W. Cole, B.F. McEwen, K.F. Buttle, and C.L. Rieder. 1997. Chromosome fragments possessing only one kinetochore can congress to the spindle equator. *J. Cell Biol.* 136:229–240.
- Khodjakov, A., R.W. Cole, B.R. Oakley, and C.L. Rieder. 2000. Centrosome-independent mitotic spindle formation in vertebrates. *Curr. Biol.* 10:59–67.
- Khodjakov, A., L. Copenagle, M.B. Gordon, D.A. Compton, and T.M. Kapoor. 2003. Minus-end capture of preformed kinetochore fibers contributes to spindle morphogenesis. *J. Cell Biol.* 160:671–683.
- Kingwell, B., and J.B. Rattner. 1987. Mammalian kinetochore/centromere composition: a 50 kDa antigen is present in the mammalian kinetochore/centromere. *Chromosoma.* 95:403–417.
- Kirschner, M., and T. Mitchison. 1986. Beyond self-assembly: from microtubules to morphogenesis. *Cell.* 45:329–342.
- Li, H.-Y., K. Cao, and Y. Zheng. 2003. Ran in the spindle checkpoint: a new function for a versatile GTPase. *Trends Cell Biol.* 13:553–557.
- Logarinho, E., H. Bousbaa, J.M. Dias, C. Lopes, I. Amorim, A. Antunes-Martins, and C.E. Sunkel. 2004. Different spindle checkpoint proteins monitor microtubule attachment and tension at kinetochores in *Drosophila* cells. *J. Cell Sci.* 117:1757–1771.
- Maddox, P., A. Straight, P. Coughlin, T.J. Mitchison, and E.D. Salmon. 2003. Direct observation of microtubule dynamics at kinetochores in *Xenopus* extract spindles: implications for spindle mechanics. *J. Cell Biol.* 162:377–382.
- Maiato, H., C.E. Sunkel, and W.C. Earnshaw. 2003. Dissecting mitosis by RNAi in *Drosophila* tissue culture cells. *Biol. Proced. Online.* 5:153–161.
- McEwen, B.F., A.B. Heagle, G.O. Cassels, K.F. Buttle, and C.L. Rieder. 1997. Kinetochore fiber maturation in PtK1 cells and its implications for the mechanisms of chromosome congression and anaphase onset. *J. Cell Biol.* 137:1567–1580.
- Megraw, T.L., L.-R. Kao, and T.C. Kaufman. 2001. Zygotic development without functional mitotic centrosomes. *Curr. Biol.* 11:116–120.
- Merdes, A., K. Ramyar, J.D. Vechio, and D.W. Cleveland. 1996. A complex of NuMA and cytoplasmic dynein is essential for mitotic spindle assembly. *Cell.* 87:447–458.
- Mitchison, T.J. 1989. Polewards microtubule flux in the mitotic spindle: evidence from photoactivation of fluorescence. *J. Cell Biol.* 109:637–652.
- Pickett-Heaps, J.D., D.H. Tippit, and K.R. Porter. 1982. Rethinking mitosis. *Cell.* 29:729–744.
- Rieder, C.L. 1991. Mitosis: towards a molecular understanding of chromosome behavior. *Curr. Opin. Cell Biol.* 3:59–66.
- Rieder, C.L., and S.P. Alexander. 1990. Kinetochores are transported poleward along a single astral microtubule during chromosome attachment to the spindle in newt lung cells. *J. Cell Biol.* 110:81–95.
- Rieder, C.L., and E.D. Salmon. 1998. The vertebrate kinetochore and its role during mitosis. *Trends Cell Biol.* 8:310–318.
- Robinson, J.T., E.J. Wojcik, M.A. Sanders, M. McGrail, and T.S. Hays. 1999. Cytoplasmic dynein is required for the nuclear attachment and migration of centrosomes during mitosis in *Drosophila*. *J. Cell Biol.* 146:597–608.
- Rogers, G.C., S.L. Rogers, T.A. Schwimmer, S.C. Ems-McClung, C.E. Walczak, R.D. Vale, J.M. Scholey, and D.J. Sharp. 2004. Two mitotic kinesins cooperate to drive sister chromatid separation during anaphase. *Nature.* 427:364–370.
- Rogers, S.L., G.C. Rogers, D.J. Sharp, and R.D. Vale. 2002. *Drosophila* EB1 is important for proper assembly, dynamics, and positioning of the mitotic spindle. *J. Cell Biol.* 158:873–884.
- Savoian, M.S., and C.L. Rieder. 2002. Mitosis in primary cultures of *Drosophila melanogaster* larval neuroblasts. *J. Cell Sci.* 115:3061–3072.
- Savoian, M.S., M.L. Goldberg, and C.L. Rieder. 2000. The rate of poleward chromosome motion is attenuated in *Drosophila* zw10 and rod mutants. *Nat. Cell Biol.* 2:948–952.
- Skibbens, R.V., C.L. Rieder, and E.D. Salmon. 1993. Directional instability of kinetochore motility during chromosome congression and segregation in mitotic newt lung cells: a push-pull mechanism. *J. Cell Biol.* 122:859–875.
- Snyder, J.A., and J.R. McIntosh. 1975. Initiation and growth of microtubules from mitotic centers in lysed mammalian cells. *J. Cell Biol.* 67:744–760.
- Spurck, T.P., O.G. Stonington, J.A. Snyder, J.D. Pickett-Heaps, A. Bajer, and J. Mole-Bajer. 1990. UV microbeam irradiations of the mitotic spindle. II. Spindle fiber dynamics and force production. *J. Cell Biol.* 111:1505–1518.
- Telzer, B.R., M.J. Moses, and J.L. Rosenbaum. 1975. Assembly of microtubules onto kinetochores of isolated mitotic chromosomes of HeLa cells. *Proc. Natl. Acad. Sci. USA.* 72:4023–4027.
- Wadsworth, P., and A. Khodjakov. 2004. E pluribus unum: towards a universal mechanism for spindle assembly. *Trends Cell Biol.* 14:413–419.
- Wilson, P., and A. Forer. 1989. The behaviour of microtubules in chromosomal spindle fibres irradiated singly or doubly with ultraviolet light. *J. Cell Sci.* 94:625–634.
- Witt, P.L., H. Ris, and G.G. Borisy. 1980. Origin of kinetochore microtubules in Chinese hamster ovary cells. *Chromosoma.* 81:483–505.
- Yu, H.-G., E.N. Hiatt, and R.K. Dawe. 2000. The plant kinetochore. *Trends Plant Sci.* 5:543–547.

Maiato et al. <http://www.jcb.org/cgi/doi/10.1083/jcb.200407090>

Materials and methods

Tubulin quantification

Western blot densitometry, using the plot profile tool in ImageJ 1.30 (National Institutes of Health, Bethesda, MD), revealed that the total tubulin pool in the S2T cell line exceeded that in control S2 cells by ~20% (see Fig. S2). For Western blots, protein extracts from 10⁶ S2 and S2T cells were resuspended in Laemmli protein sample buffer and were separated according to their molecular weights by SDS-PAGE. After transferring proteins to nitrocellulose membranes (Amersham Biosciences), α-tubulin was detected with a mouse mAb diluted 1:10,000 (clone B512; Sigma-Aldrich) as described previously (Maiato et al., 2002).

Quantification of the mitotic phenotype after dynein RNAi

Drosophila S2T cells were grown on poly-L-lysine-coated coverslips. After 3 d in dynein RNAi, they were fixed with 4% PFA. After staining of DNA with DAPI, the coverslip cultures were mounted on glass slides in Vectashield (Vector Laboratories) for fluorescence analyses. Protein depletion by RNAi was monitored by Western blotting, as described previously (Maiato et al., 2003), using the mouse monoclonal P1H4 anti-dynein heavy chain antibody (McGrail and Hays, 1997). Mitotic index in untreated and in dynein RNAi-treated cultures was determined visually, and was scored as the average percentage of mitotic cells, in total populations of 1,497 and 1,533 cells, respectively. Total cell numbers were derived from three independent experiments.

Determination of interkinetochore distances during metaphase in the presence or absence of tension

To determine the interkinetochore distances during metaphase in *Drosophila* S2T cells, we performed immunofluorescence analysis with chicken anti-Cid (CENP-A orthologue in *Drosophila*) antibodies (Blower, and Karper, 2001). For this purpose, we allowed S2T cells to adhere for 2 h to Con A-treated coverslips (Goshima and Vale, 2003) and performed the immunoflu-

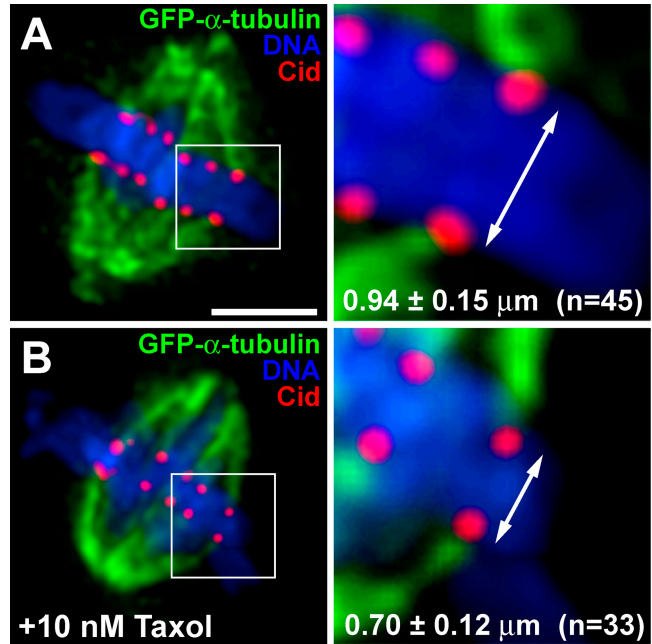
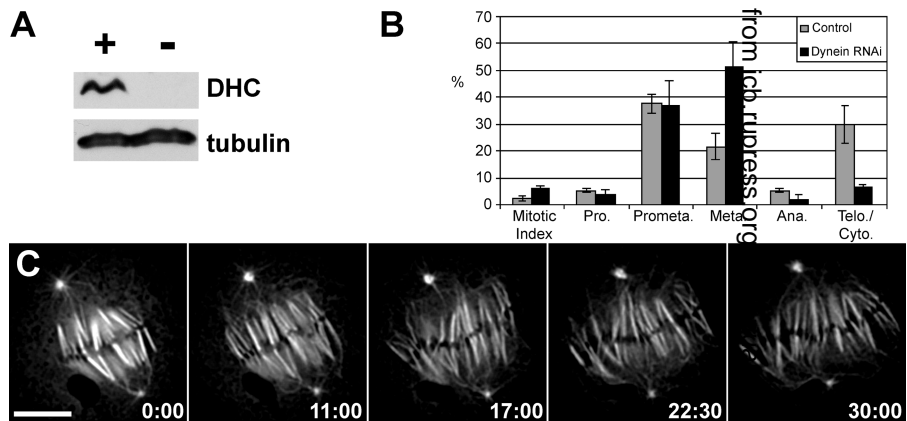


Figure S1. Taxol treatment decreases distances between sister kinetochores in *Drosophila* S2 cells. S2T cells were fixed and immunostained with anti-CID (*Drosophila* CENP-A orthologue). DNA was counterstained with Hoechst 33342. Interkinetochore distance was measured as the distance between the centroids of the CID-positive structures on opposite sides of a chromosome. (A) Maximal-intensity projection of a typical control S2 cell during metaphase. (B) Maximal-intensity projection of a typical cell after a 10-min incubation with 10 nM taxol. Average interkinetochore distance values and number of measurements are shown. Bar, 5 μm.

Depletion efficiency and mitotic characterization after dynein RNAi.

(A) Western blot showing that cytoplasmic dynein heavy chain is undetectable after RNAi. Endogenous α-tubulin is shown as a loading control. (B) Determination of the mitotic index and respective distribution of mitotic stages after dynein RNAi. Depletion of dynein caused a slight increase of mitotic cells that accumulated in metaphase. (C) Selected sequences from a time-lapse recording of a metaphase cell with a bipolar spindle, whose K-fibers splay out near the poles in the absence of dynein. Bar, 5 μm.



orescence protocol as described previously (Maiato et al., 2003). 3-D datasets were collected with a DeltaVision system equipped with a CM350 CCD camera (Photometrics) based on an inverted light microscope (model IX70; Olympus); they were subsequently deconvolved using SoftWorx 2.5 (Applied Precision). Images were processed for publication using Photoshop 6.0 (Adobe Systems). To decrease tension at metaphase kinetochores, we treated S2T cells with 10 nM taxol for 10 min as described previously (Logarinho et al., 2004). Interkinetochore distances in the absence or presence of taxol were determined by measurement of centroid positions from CID-labeled kinetochores from three individual cells for each case, using SoftWorx 2.5.

References

- Blower, M.D., and G.H. Karper. 2001. The role of *Drosophila* CID in kinetochore formation, cell-cycle progression and heterochromatin interactions. *Nat. Cell Biol.* 3:730–739.
- Goshima, G., and R.D. Vale. 2003. The roles of microtubule-based motor proteins in mitosis: comprehensive RNAi analysis in the *Drosophila* S2 cell line. *J. Cell Biol.* 162:1003–1016.
- Logarinho, E., H. Bousbaa, J.M. Dias, C. Lopes, I. Amorim, A. Antunes-Martins, and C.E. Sunkel. 2004. Different spindle checkpoint proteins monitor microtubule attachment and tension at kinetochores in *Drosophila* cells. *J. Cell Sci.* 117:1757–1771.
- Maiato, H., P. Sampaio, C.L. Lemos, J. Findlay, M. Carmena, W.C. Earnshaw, and C.E. Sunkel. 2002. MAST/Orbit has a role in microtubule-kinetochore attachment and is essential for chromosome alignment and maintenance of spindle bipolarity. *J. Cell Biol.* 157:749–760.
- Maiato, H., C.E. Sunkel, and W.C. Earnshaw. 2003. Dissecting mitosis by RNAi in *Drosophila* tissue culture cells. *Biol. Proced. Online.* 5:153–161.
- McGrail, M., and T.S. Hays. 1997. The microtubule motor cytoplasmic dynein is required for spindle orientation during germline cell divisions and oocyte differentiation in *Drosophila*. *Development.* 124:2409–2419.

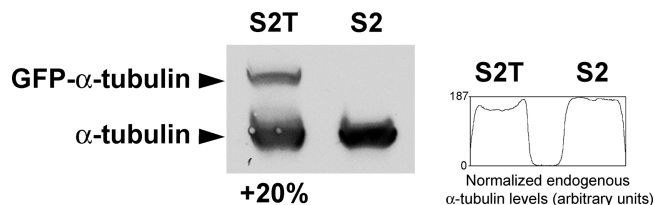


Figure S3. **Quantification of the total α -tubulin levels present in the stable cell line expressing GFP/ α -tubulin.** Western blot with an anti- α -tubulin antibody showing the levels of endogenous and chimeric GFP/ α -tubulin in control S2 and S2-GFP/ α -tubulin (S2T) cell lines. A protein extract from 10^6 cells was loaded on each lane. Note the presence of an additional small pool of GFP- α -tubulin in the S2T cell line. Interestingly, the levels of endogenous α -tubulin are slightly lower in S2T cells than in S2 cells (see densitometry plot on the right). This likely represents a feedback inhibition control mechanism, caused by the ectopic expression of functional GFP/ α -tubulin on the endogenous α -tubulin pool. Overall, the total α -tubulin pool (endogenous + ectopic) of the S2T cell line exceeds by $\sim 20\%$ the endogenous α -tubulin levels in control S2 cells.